Electronic Supplementary Material (ESI) for Chemical Communications

Resolution of a paradox by native mass spectrometry: facile occupation of all four binding sites in the dimeric zinc sensor SmtB

Frances D. L. Kondrat, Gregory R. Kowald, Charlotte A. Scarff, James H. Scrivens and Claudia A. Blindauer

Supplementary Material

Molecular modelling of Zn_4SmtB_2

The model presented in Figure 1 is based on pdb file 1r23,[1] which pertains to dimeric wild-type SmtB with one Zn ion per dimer. This structure was the most suitable template for our purposes, as at least for one of the monomers, all residues from His18 to Cys121 are resolved in the structure, whereas all other available structures suffer from more missing residues. It should be noted though that the mutual orientation of the monomers in α5-Zn_2SmtB_2 is slightly different from our model.

To create an SmtB structural model with two ocupied αN3 sites, first the N-terminus of the second monomer (B), in which residues 18-24 were not resolved, was extended, making use of coordinates derived from monomer A. Subsequently, we employed the homology modelling program MODELLER (v. 9.7)[2] to further extend both N-termini up to Val13. The 10 models generated were inspected manually, and we chose one that showed the two extensions in the most frequently observed conformation. Side-chain conformations, with the exception of those of Asp104, His106, His117, and Glu120 (the α5 ligands) were optimised using SCWRL (v. 3.0).[3] Subsequently, the model was imported into the program MOE (v. 2.0), hydrogens were added, and four Zn ions were introduced into the four sites. Each site was then energy-minimised separately, using a customised version of the AMBER force-field, in which we have incorporated Zn-specific parameters as well as increasing the restraint on omega-angles, which we had found to be unsatisfactory in the original version. After energy-minimisation of the position of the immediate ligands, the adjacent environment was optimised, and finally, the entire molecule was subjected to energy minimisation. All minimisations were terminated based on the steepness of the RMS gradient (<0.05). The final model was then submitted to the WHATIF web interface,[4] ensuring that a physically reasonable model had been produced.

Experimental Methods

Protein expression and purification *E. coli* cells transformed with plasmid Psrk15-1 (donated by N.J. Robinson, Durham University) were grown overnight. A single colony was grown up, under antibiotic resistance, and induced to over express SmtB. Harvested bacterial pellets were sonicated producing a cell lysate. The filtered lysate was purified by heparin affinity and size exclusion chromatography and then lyophilised for storage at -80 °C.

Inductively coupled plasma optical emission spectroscopy For ICP-OES measurements, samples were re-suspended in 20 mM ammonium bicarbonate and diluted 5-fold into 0.1 M nitric acid. Zinc, sulfur, cadmium and copper standards at 0, 0.2, 0.5, 0.7 1.0 and 2.0 ppm were used for calibration. Samples that had undergone ultrafiltration (10 kDa cut-off) were also measured; neither increase nor reduction in Zn:protein ratio was observed.

Electrospray ionisation mass spectrometry For ESI-MS measurements, lyophilised SmtB samples were dissolved in 10 mM ammonium bicarbonate and then further washed and desalted by centrifugation. Millipore centrifuge columns (10 kDa cut-off) were used with an average of five spins required for sufficient salt removal. The pH of buffers and samples was adjusted using ammonia or acetic acid. All samples were loaded into fused silica nanospray needles and introduced into the ESI source. Experiments were conducted on a Synapt HDMS system (Waters Corporation). Spraying conditions were optimised in ESI positive mode scanning between 500-3500 *m/z*. The optimal instrument parameters were found to be; capillary voltage, 1.2 kV, source temperature, 90 °C and cone voltage, 60 V. A 1 mg/ml Caesium iodide solution (50 % isopropanol) was used to calibrate the time of flight (TOF) mass analyser, to ensure accurate masses were obtained. MassLynx V4.1 software was used for the acquisition of data.

To obtain the molecular masses of the SmtB species, mass spectra were deconvoluted onto a true mass scale using maximum entropy modeling software.

Reaction with EDTA Desalted SmtB samples were concentrated to 0.8 mM monomer concentration and incubated, at room temperature, with 1.6 mM EDTA. For this purpose, H_4EDTA (Sigma-Aldrich) was neutralised by the addition of 4 mol eq. of aqueous ammonia. At selected time points, aliquots of the reaction mixture were taken and diluted to approximately 10 μM in a mass spectrometry compatible buffer (10 mM ammonium bicarbonate pH 7.4) before being loaded into a nanospray needle. ESI-MS measurements were then carried out under the conditions described above.

Collisionally induced dissociation A desalted 13 μM sample of SmtB in 10 mM ammonium bicarbonate pH 7.4 was infused via nanospray needles into the mass spectrometer. The mass spectrometry conditions applied were identical to those outlined above. The cone voltage was maintained at 60 V, whilst the trap collision energy (CE) was ramped from 4 V to 55 V.

Electron transfer dissociation Electron transfer dissociation (ETD) experiments were carried out, by Dr. Juilia Smith, on an amaZon speed ETD system (Bruker, Coventry, UK). A Zn_4SmtB_2 sample was desalted/cleaned as indicated previously and was diluted, using 10 mM ammonium bicarbonate (pH 7.4) to 2 ρmol/μL. This sample was then infused, from a syringe drive, into the system at 3 μL/min. Intact masses were determined using UltraScan mode and MaxEnt deconvolution. The isolation of both monomeric and dimeric SmtB with differing numbers of zinc ions bound was conducted prior to ETD fragmentation in conjunction with proton transfer reaction (PTR). Flouranthene radical anions and Flouranthene anions, which are generated in a negative chemical ionization source, were used as the ETD and PTR reagents respectively. ETD ion charge control (ICC) was 250000 with an 8 ms reaction time, whilst PTR ICC was 150000 with a 20 ms reaction time. Compass Data Analysis 4.0 was used in conjunction with BioTools 3.2 and Sequence Editior 3.2 to analyse spectra to determine sequence coverage.

Table S1. Theoretical and experimental masses for SmtB species in the absence of EDTA. The masses of all observed species were within ± 0.2 Da of the expected masses. This indicates that there was no significant disulfide bond formation within SmtB.

Monomeric SmtB	Expected mass (Da)	Observed mass (Da)	Mass difference
Zn_2	13540.1	13540.0	-0.1
Zn	13476.7	13476.5	-0.2
Apo	13413.3	13413.5	0.2

Dimeric SmtB	Expected mass (Da)	Observed mass (Da)	Mass difference
Zn_4	27080.2	27080.0	-0.2

Table S2. Theoretical and experimental masses for SmtB species after incubation with EDTA for 3 hours. The masses of all observed species were within ± 0.7 Da of the expected masses of SmtB.

Monomeric SmtB	Expected mass (Da)	Observed mass (Da)	Mass difference
Zn_2	13540.1	13540.0	-0.1
Zn	13476.7	13477.0	0.3
Apo	13413.3	13414.0	0.7

Dimeric SmtB	Expected mass (Da)	Observed mass (Da)	Mass difference
Zn_4	27080.2	27079.5	-0.7
Zn_3	27016.8	27016.5	-0.3
Zn_2	26953.4	26953.0	-0.4
Zn	26890.0	26889.5	-0.5
Apo	26826.6	26826.0	-0.6

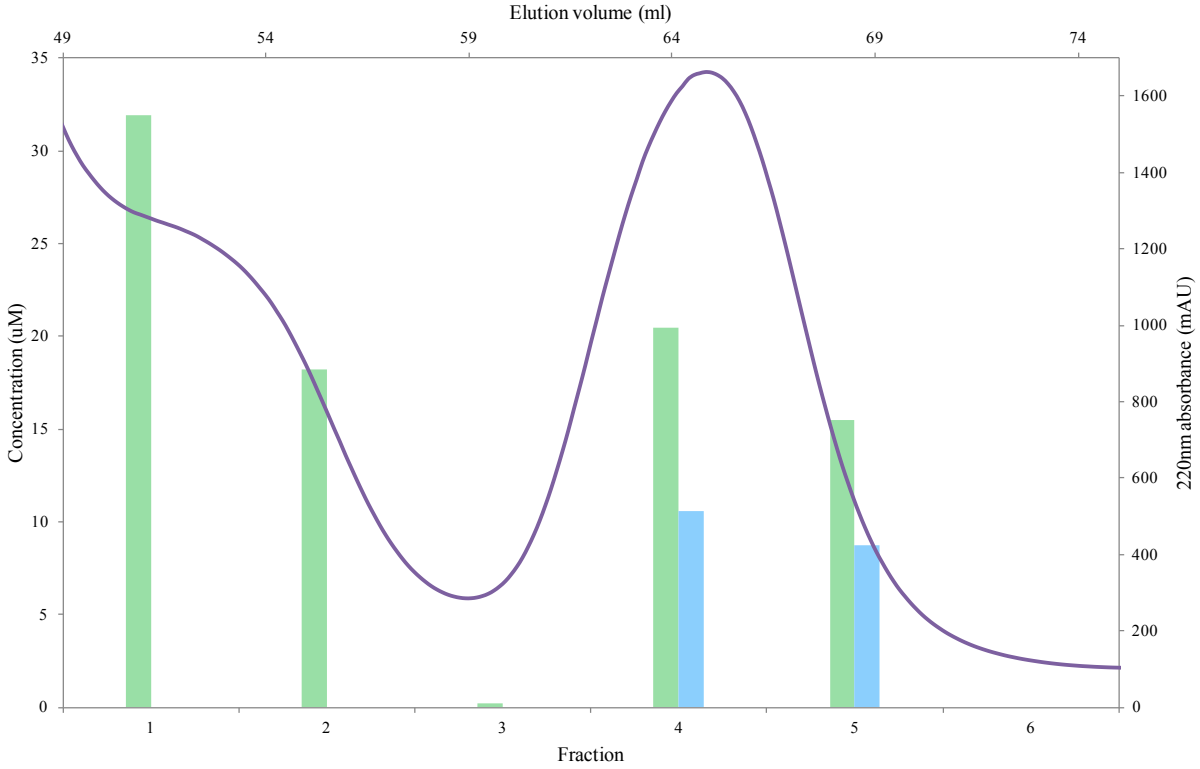

Figure S1. Second purification step of zinc-loaded SmtB, after capture of Zn-loaded SmtB on a heparin column. An average of two gel filtration chromatograms, as monitored by absorbance at 220 nm (purple line) is overlaid with the concentrations of sulphur (green) and zinc (blue), within the displayed fractions. Fractions 4 and 5 correspond to SmtB, and the Zn:S ratio, as determined by ICP-OES, was 1.6:3 (±0.2).

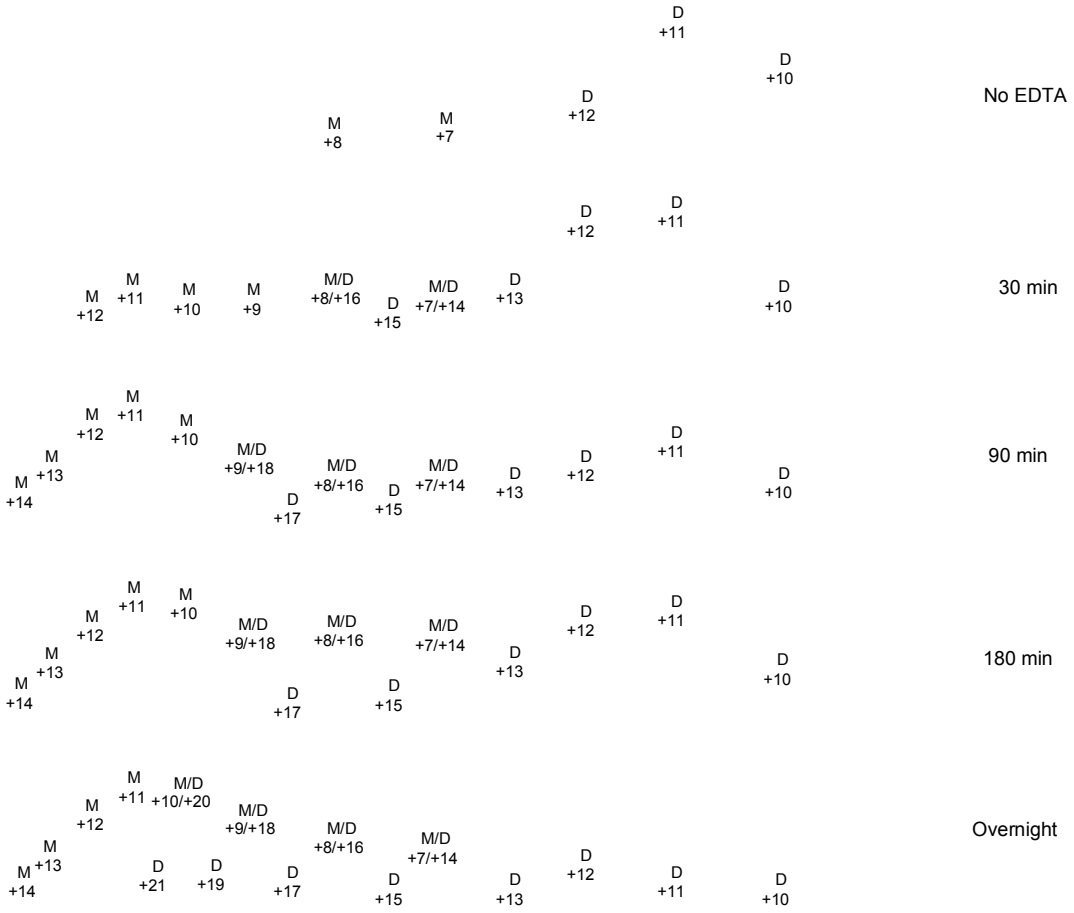

Figure S2. ESI mass spectra of 0.8 mM SmtB in 10 mM ammonium bicarbonate pH 7.4 during reaction with 1.6 mM EDTA. A decrease in the relative abundance of dimeric species and an increase in the relative abundance of monomeric species can be clearly observed. A close-up of the +11 charge state for the dimers is shown in Figure S3.

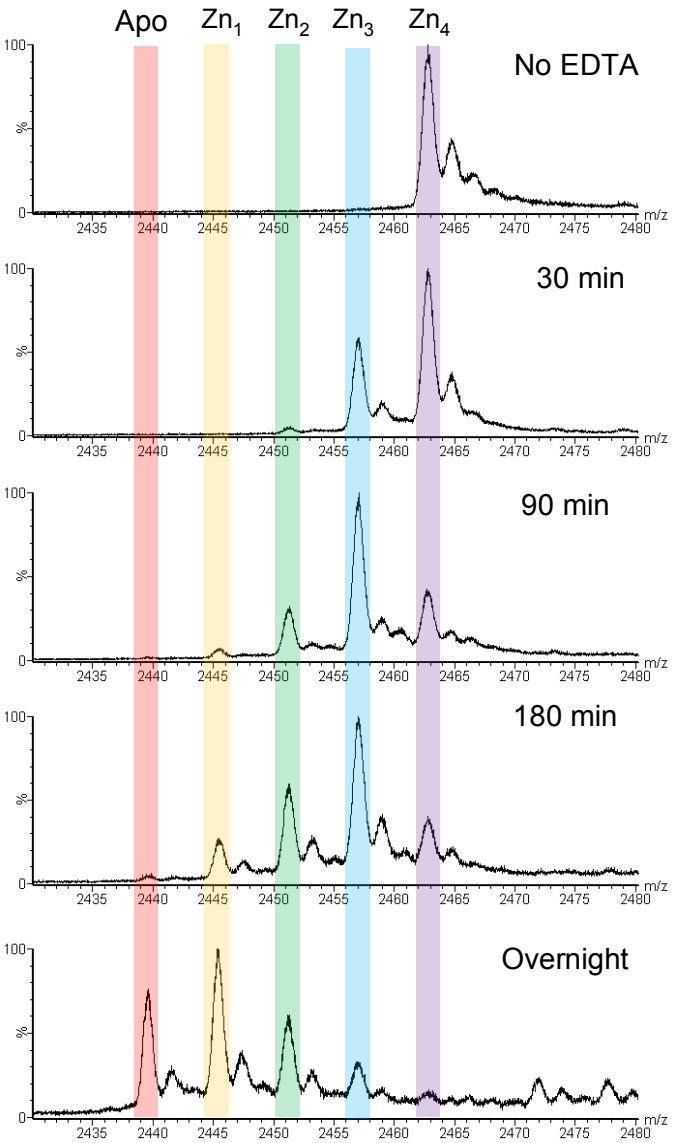

Figure S3. The +11 charge state for dimeric SmtB species during the reaction with equimolar EDTA. The reaction of Zn-SmtB with EDTA is relatively slow, and all five possible species can be observed. Zinc ions are removed in a step-wise fashion one by one, with no preference for any particular intermediate.

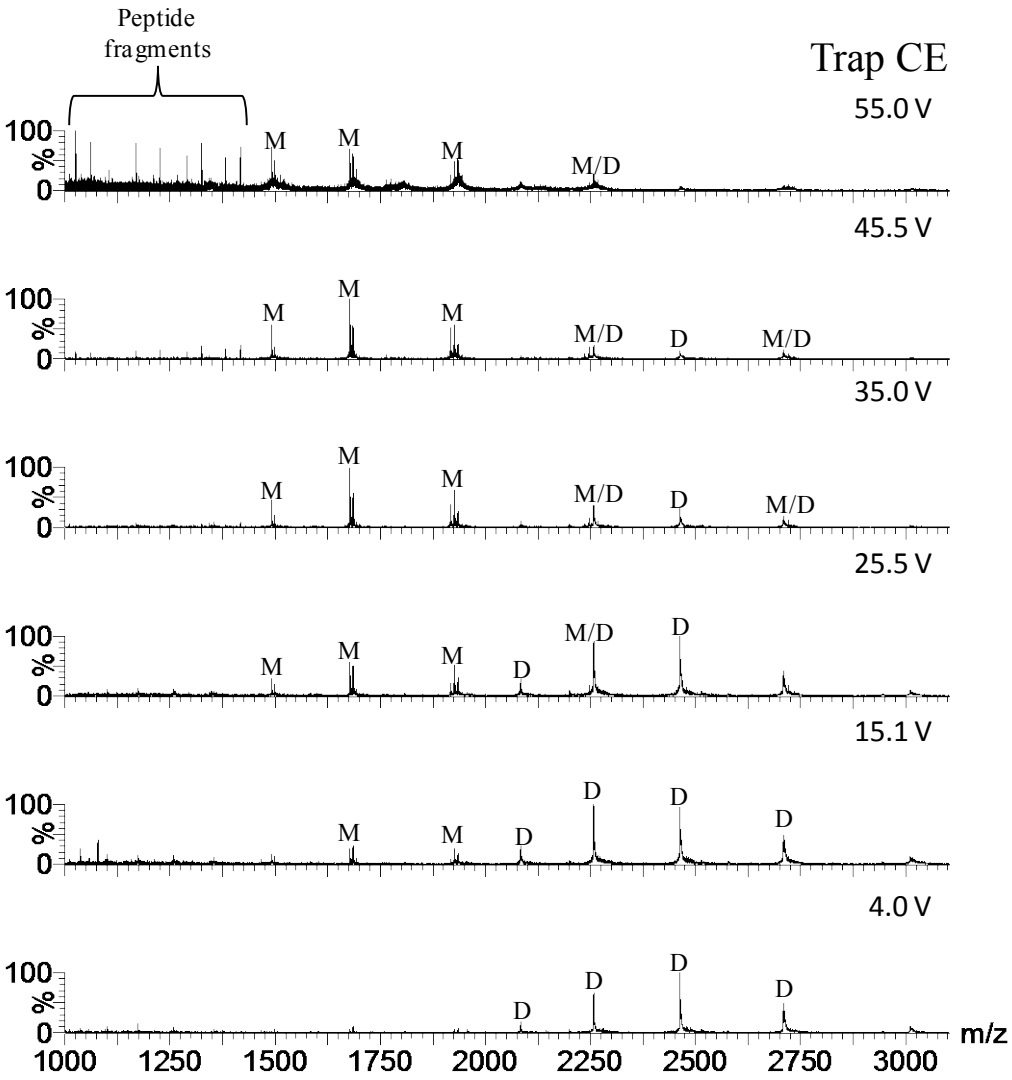

Figure S4. Collisionally induced dissociation of a native SmtB sample in 10 mM ammonium bicarbonate. Monomeric (M) and dimeric (D) charge states are labelled and peptide fragments are indicated. Increasing trap voltage used in collisionally induced dissociation (CID) led to dissociation of the dimer as well as loss of zinc ions, followed by fragmentation. CID generated fragments throughout the sequence of SmtB (Table S3), however the majority of fragments were identified to belong to the flexible N-terminal region. To double-check for eventual Zn-containing fragments, the *m/z* values of the fragments identified to contain partial zinc binding sites were recalculated with the addition of a single zinc ion and the raw data was interrogated for the resulting values. No fragments were found to be in association with zinc ions.

Table S3. The peptides produced from CID and the position of those peptides within the SmtB sequence. Residues involved in zinc ion binding are highlighted in red. All non-y type ions were converted to y-type ions as described in the literature[5] and are indicated by a *.

Observed Mass $[M+H]^+$ (Da)	Predicted Mass $[M+H]^+$ (Da)	Δ Mass (Da)	Peptide	Position
2067.1*	2067.54	-0.046	TKPVLQDGETVVCQGTHAAI(A)	2-21
2120.1	2120.091	-0.009	(A)SELQAIAPEVAQSLAEFFAV(L)	23-42
2207.1	2207.122	0.012	(V)VCQGTHAAIASELQAIAPEVAQ(S)	13-34
2294.1	2294.144	0.044	(V)VCQGTHAAIASELQAIAPEVAQS(L)	13-35
2294.1	2294.221	0.121	(V)GDLAQAIGVSESAVSHQLRS LR(N)	63-84
2336.2	2336.285	0.084	(L)RNLRLVSYRKQGRHVYYQ(L)	85-102
2392.2*	2392.317	0.116	(L)AQAIGVSESAVSHQLRSLRN LR(L)	66-87
2449.3	2449.369	0.068	(S)LRNLRLVSYRKQGRHVYYQ(L)	83-101
2449.3	2449.369	0.068	(L)RNLRLVSYRKQGRHVYYQL(Q)	84-102
2506.3	2506.297	-0.003	(T)VVCQGTHAAIASELQAIAPEVAQSL(A)	12-36
2577.3	2577.263	-0.036	(R)HVYYQLQDHHIVALYQNALDH(L)	97-117
2577.3	2577.334	0.034	(T)VVCQGTHAAIASELQAIAPE VAQSLA(E)	12-37
2577.3	2577.427	0.127	(L)RNLRLVSYRKQGRHVYYQLQ(D)	84-103
2603.4	2603.360	-0.039	(A)IASELQAIAPEVAQSLAEFF AVLAD(P)	21-45
2666.41*	2666.345	-0.064	TKPVLQDGETVVCQGTHAAI ASELQA(I)	2-27
2666.41*	2666.359	-0.051	(K)QGRHVYYQLQDHHIVALYQNAL(D)	94-115
2713.31*	2713.492	0.181	(R)LRLLSLLARSELCVGDLAQA IGVSES(A)	49-74
2779.51*	2779.429	-0.080	TKPVLQDGETVVCQGTHAAIASELQAI(A)	2-28
2779.51*	2779.581	0.071	(S)HQLRSLRNLRLVSYRKQGRH VY(Y)	78-99
2821.51*	2821.404	-0.106	(V)LQDGETVVCQGTHAAIASEL QAIAPEVA(Q)	6-33
2832.5	2832.580	0.080	(G)DLAQAIGVSESAVSHQLRSL RNLRLV(S)	64-89

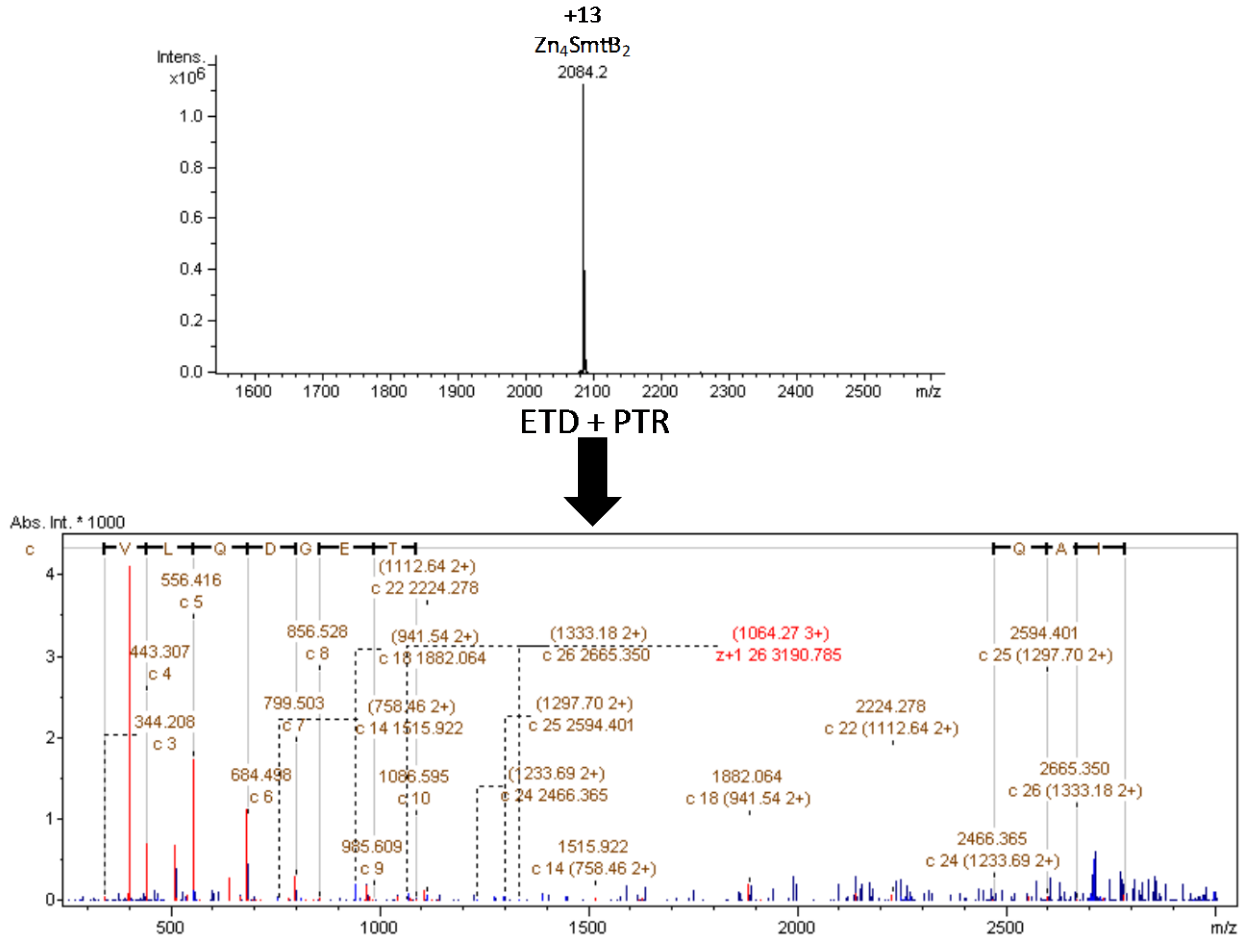

Figure S5. Isolation and subsequent ETD/PTR fragmentation of the +13 charge state of Zn_4SmtB_2 (2084.2 *m/z*) yielding low sequence coverage and no observable Zn-bound fragments.

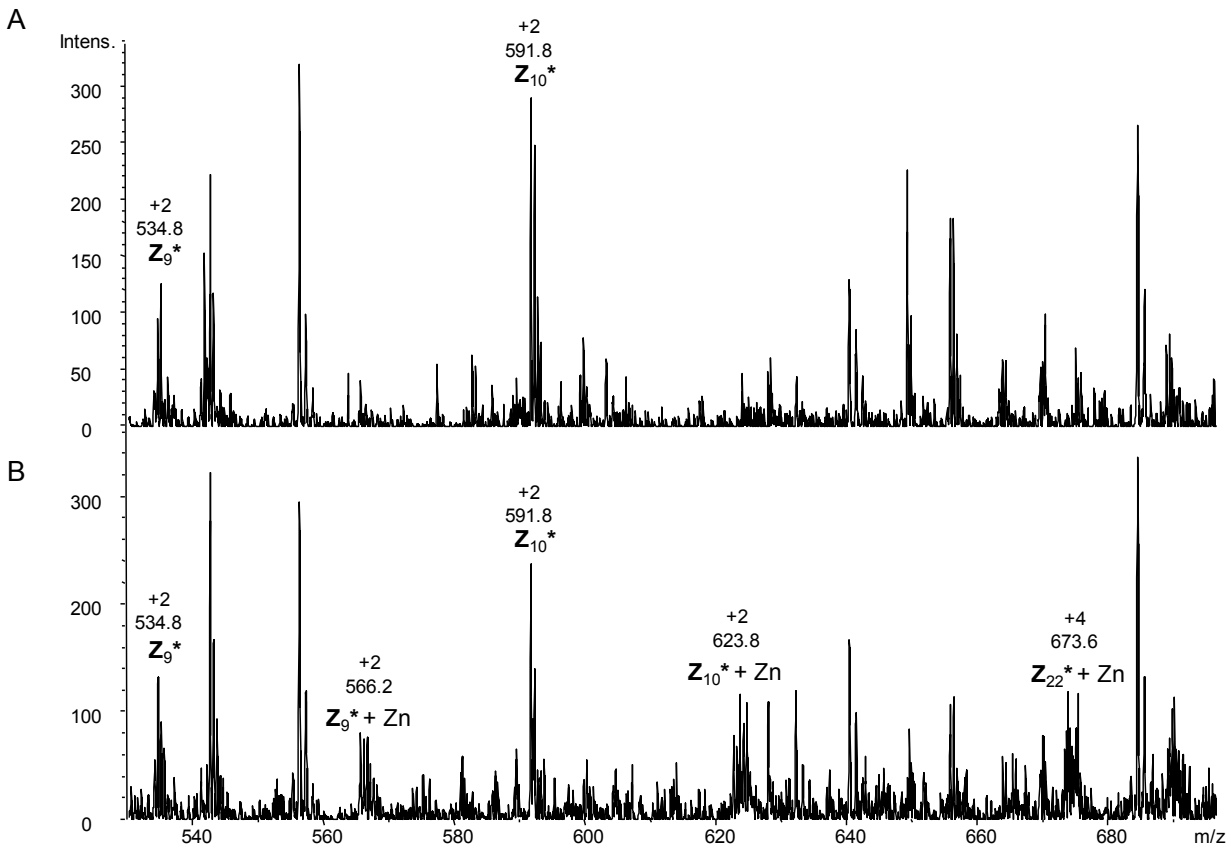

Figure S6. ETD/PTR spectra of the +15 charge state of A) apo-SmtB 895.3 *m/z* and B) Zn_2SmtB 903.8 m/z (also see Figure S7). Labels indicate apo or zinc loaded Z* (Z+1) fragments. The majority of the Zn-containing fragments observed from the ETD/PTR reactions on the +15 charge state of Zn_2SmtB were Z+1 ions from the C-terminus of the protein. The α5 zinc binding site is known to be located within this region of SmtB with X-ray crystallography studies identifying the zinc binding ligands as H117, E120 from one monomer and H106 and D104 from the opposing monomer. All the identified zinc bound fragments contained either all four of these residues, such as $Z+1_{22}$ or at least a partial α5 zinc binding site, $Z+1_9$ and $Z+1_{10}$, confirming that a zinc binding site is located within this region.

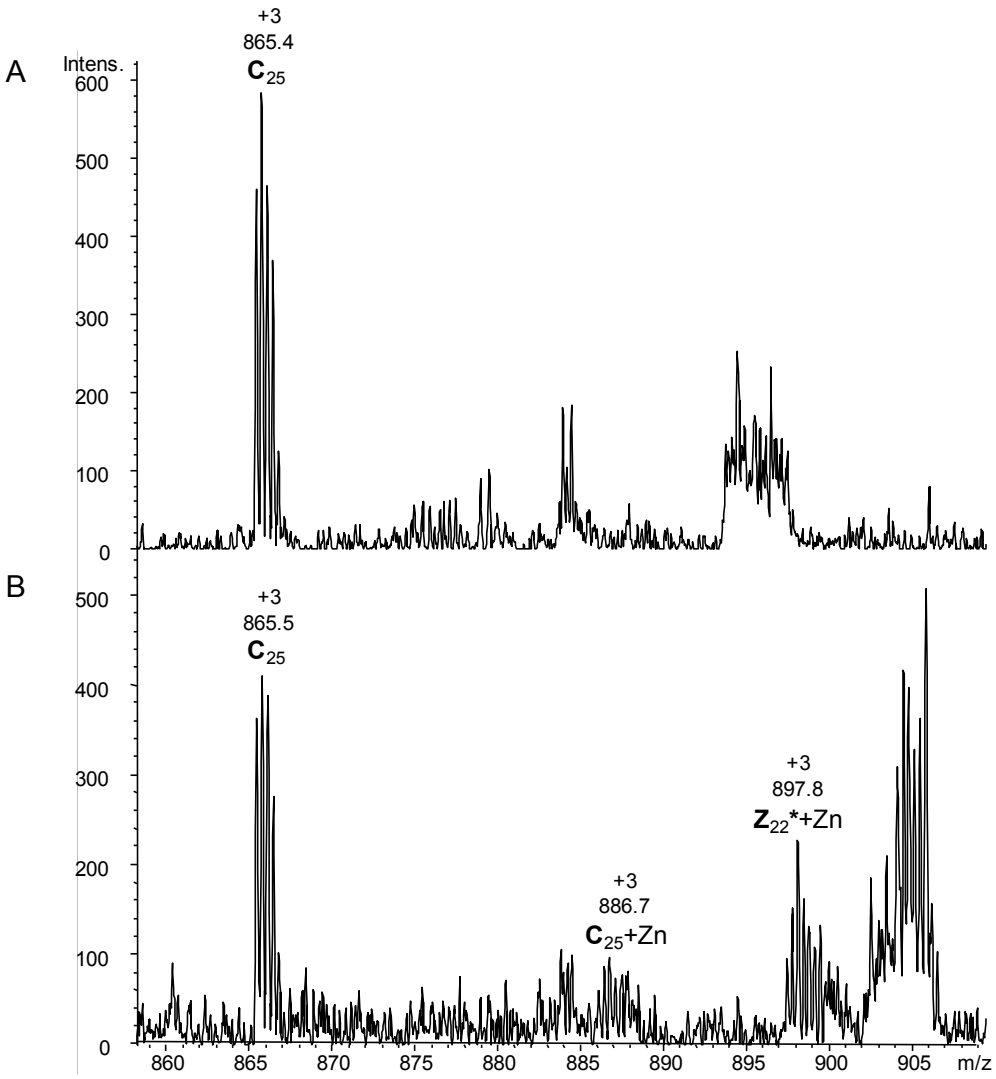

Figure S7. ETD/PTR spectrum of the +15 charge state of A) apo-SmtB 895.3 *m/z* and B) Zn_2SmtB 903.8 m/z, zoomed on a region containing a possible Zn-containing fragment from the N-terminus $(C_{25}+Zn)^{3+}$. Labels indicate apo and zinc loaded Z* (Z+1) or C fragments. The non-sensory αN3 zinc binding site has not been characterised crystallographically, however there is evidence to suggest that C14, H18 from the N-terminal arm of one monomer forms a tetrahedral binding site with C61 and D64 from the α3 helix of the other monomer. X-ray structures with incorporated mercury ions, predicted to mimic zinc ion binding, identified C61 and D64, along with His 97 and a water molecule to make up the α3N site.[6] These early data have been revised after more recent NMR perturbation data showed large backbone movements to the C61, D64 and C14 residues upon zinc addition to apo-$SmtB_2$.[7] Site-dreceted mutagenesis and optical absorption spectroscopy using Co(II) as a zinc binding probe supported the involvement of both C14 and C61 within the α3N binding site [3]. In the current experiments, a number of fragments of the N-terminus were identified, but only a single C ion was observed to have a possible zinc ion attached. The C61 and D64 residues are probably buried too deeply within the protein's tertiary structure to be able to obtain sufficient fragmentation within this region. The observed C_{25} fragment does however contain the C14 and H18 residues and re-empathizes their probable involvement in zinc ion ligation, although the signal to noise ratio of this peak is too low to be conclusive.

References

1. C. Eicken, M. A. Pennella, X. H. Chen, K. M. Koshlap, M. L. VanZile, J. C. Sacchettini and D. P. Giedroc, *J Mol Biol*, 2003, **333**, 683-695.

2 M. A. Marti-Renom, A. C. Stuart, A. Fiser, R. Sanchez, F. Melo and A. Sali, *Annu. Rev. Biophys. Biomol. Struct*., 2000, **29**, 291–325.

3 A. A. Canutescu, A. A. Shelenkov, and R. L. Dunbrack, Jr., *Protein Sci.*, 2001, **12**, 2001-2014.

4 http://swift.cmbi.ru.nl/servers/html/index.html.

5 A. Armirotti, U. Benatti and G. Damonte, *Rapid Commun. Mass Spectrom.*, 2009, **23**, 661-666.

6 W. J. Cook, S. R. Kar, K. B. Taylor and L. M. Hall, *J. Mol. Biol.*, 1998, **275**, 337-346.

7 M. L. VanZile, X. H. Chen and D. P. Giedroc, *Biochemistry* 2002, **41**, 9765-9775.